

## Supplementary Information

### **Synthesis of Optically Tunable Bumpy Silver Nanoshells by Changing the Silica Core Size and Their SERS Activities**

*Hyejin Chang, Eunbyeol Ko, Homan Kang, Meong Geun Cha, Yoon-Sik Lee\* and Dae Hong Jeong\**

#### **List of Contents**

1. **Table S1** Comparison of the synthesis of bumpy AgNSs using different Si NPs with diameters of 170-nm and 40-nm as core particles.
2. **Table S2** Controlling the surface area of Si NPs of various sizes for Si NP for Ag shell formation.
3. **Fig. S1** Comparison of synthesis of bumpy AgNSs using different Si NPs with diameters of 170-nm and 40-nm as core particles.
4. Details in the optimization of fabrication processes for non-aggregated AgNSs of various sizes.
5. **Fig. S2** Optimization of synthesis of AgNS with a 40-nm Si NP core.
6. **Table S3** Detailed structures of AgNSs by Si NP core sizes.
7. **Fig. S3** Measurements of diameters of Ag NPs on AgNSs.
8. **Fig. S4** The evaluation method of the roughness factor of AgNSs.
9. **Fig. S5** The size distributions of 4-FBT labeled AgNS (I)-(V) measured by Nanoparticle Tracking Analysis (NTA).
10. **Fig. S6** Analysis of SERS properties of AgNSs in solution with different excitation lasers.
11. Details of calculation of the SERS enhancement factor (EF)
12. **Table S4** The size of Ag NP assembled on Si NP core and calculation of roughness elements from bumpy AgNS particles.
13. **Fig. S7** The TEM image of AgNS (I). Black circles indicate aggregation of particles.
14. References in Supplementary Information.

**Table S1.** The detailed condition used in the synthesis of Si NPs of various sizes. (mean±S.D., n=20)

<b>Size (nm)</b>	<b>Triton-X</b>	<b>1-Hexanol</b>	<b>Ammonia</b>
42.0 ± 2.6	1.88 g	1.6 mL	100 µL
59.3 ± 3.9	1.88 g	1.6 mL	75 µL
82.0 ± 12.3	2.4 g	1.8 mL	100 µL
103.0 ± 12.0	1.88 g	1.6 mL	60 µL

**Table S2.** Controlling the surface area of Si NPs of various sizes for Ag shell formation. The relative surface areas per unit mass were different according to the size of Si NP as shown in this table, and the reacting surface areas of Si NPs were controlled equally as 320 cm<sup>2</sup> by adjusting a number of silica nanoparticles.

(per reaction batch, 30 mg of AgNO<sub>3</sub>)

<b>Sample name</b>	<b>Si NP size (nm)</b>	<b>Relative Surface areas per unit mass to 147.9 nm Si NP</b>	<b>Reacting mass of Si NP (mg)</b>	<b>Reacting surface area of Si NP (cm<sup>2</sup>)</b>
-	42.0	3.73	<b>0.5</b>	320
Si NP (i)	59.3	2.51	<b>0.8</b>	320
Si NP (ii)	82.0	1.80	<b>1.1</b>	320
Si NP (iii)	103.0	1.44	<b>1.4</b>	320
Si NP (iv)	123.7	1.20	<b>1.7</b>	320
Si NP (v)	147.9	1	<b>2.0</b>	320

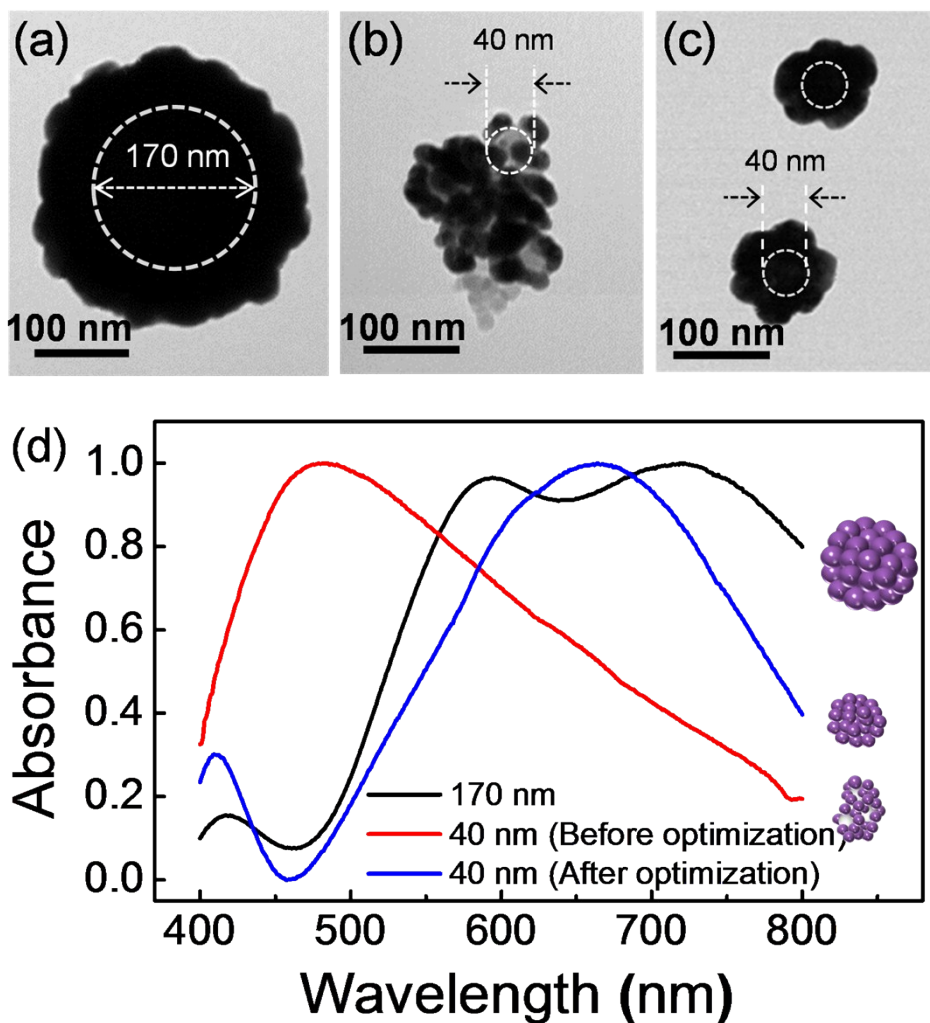


**Fig. S1.** Comparison of the synthesis of bumpy silver nanoshells (AgNSs) using different silica nanoparticles (Si NPs) with a diameter of 170-nm and 40-nm as core particles. TEM images of synthesized Ag NS with (a) 170-nm Si NP and (b) 40-nm Si NP under the same synthetic conditions. (c) TEM images of AgNSs using 40-nm Si NP after optimizations (Figure S2) (d) UV-Vis extinction spectra (normalized) of the AgNSs of (a) – (c).

## **Optimization of fabrication processes for non-aggregated AgNSs in various sizes**

To address the aggregation problem in the fabrication processes, the reaction condition was modified by using different alkylamines instead of octylamine, and varying the amounts of  $\text{AgNO}_3$ , PVP, and the silica core. First, the amount of Si NP was reduced, which decreased the reacting surface for avoiding aggregation of Si NPs, and also increased the relative amount of precursor ( $\text{Ag}^+$ ) for complete formation of silver nanoshells. While the reduced amount of Si NP from 2 mg to 0.5 mg led to successful fabrication of AgNS; however, using less than 0.5 mg amount of Si NP resulted in the thick layer of silver shell. Because an excessive amount of  $\text{AgNO}_3$  compared to Si NP causes for Ag NPs to overgrow on the surface of Si NP, the final size was much larger than the size of the core (the shell was too thick). Consequently, when we used less than 0.5 mg, using 40-nm sized Si NP core would be meaningless. Second,  $\text{AgNO}_3$  was used with the same amount as the condition using 170-nm Si NP. We tried to use less than a 30-mg amount of  $\text{AgNO}_3$  to prevent the emergence of excessive amounts of Ag NPs in solution, but the formation of the silver nanoshell was incomplete. Third, the amount of PVP as a dispersing agent was increased from 5 mg to 10 mg to prevent aggregation and to fabricate homogeneous AgNSs. Fabricated AgNSs appeared similar, irrespective of whether 10 mg or more of PVP was used in the process. Last, the kind of reducing agent was changed from octylamine to ethanolamine. The hydroxyl group of ethanolamine is an electron-withdrawing group, and consequently, the amine group of ethanolamine serves as a weaker electron-donating group to silver ion because of the inductive effect of the hydroxyl group. The size of AgNP assembled on the silica core was smaller when using ethanolamine compared to using octylamine, because  $\text{Ag}^+$  cannot be efficiently reduced to  $\text{Ag}^0$  with ethanolamine.<sup>1</sup>

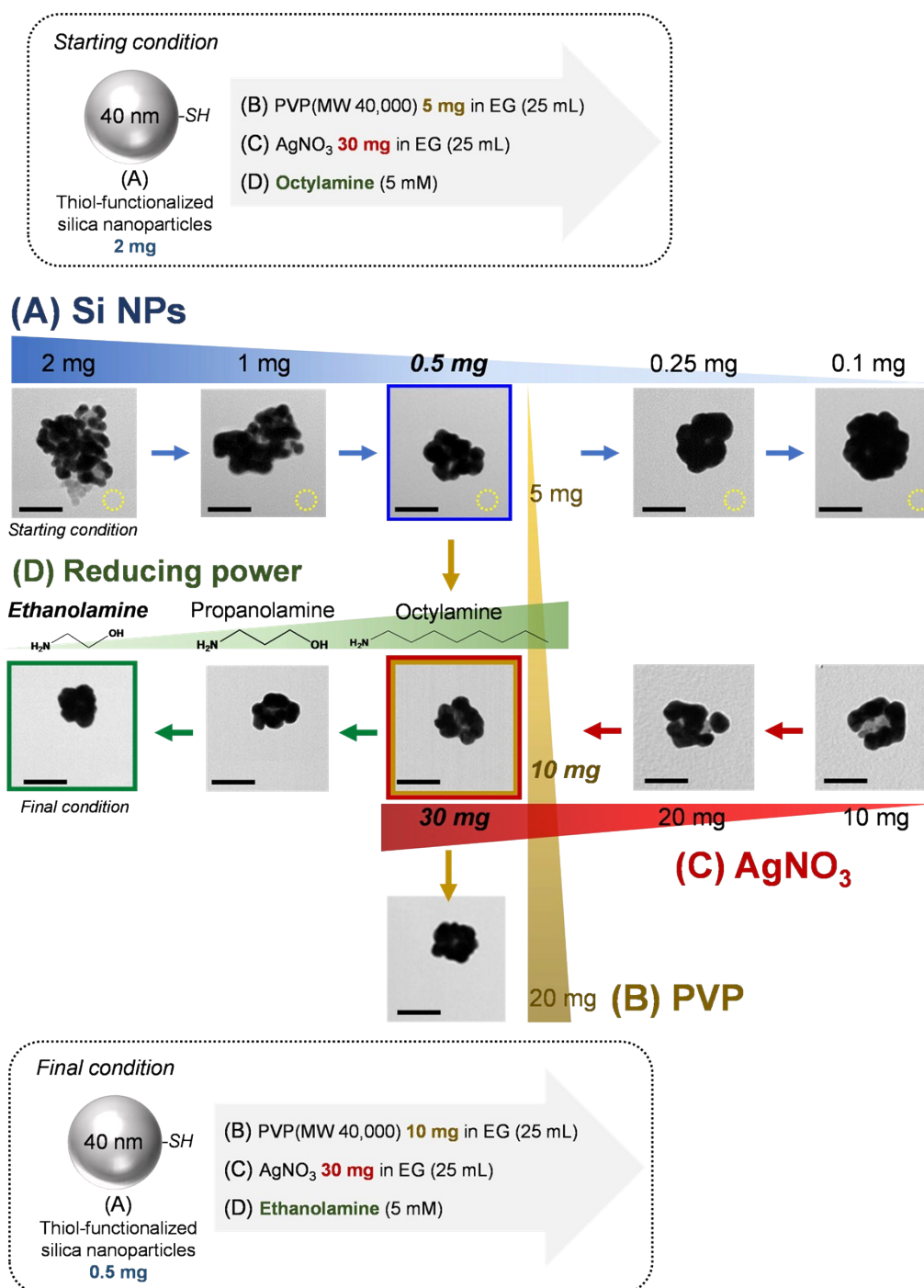


**Fig. S2.** Optimization of synthesis of AgNS with the 40-nm Si NP core. One variable changed under the starting conditions. Outlined images indicate the optimized synthetic conditions. (A) The amount of Si NPs was reduced first, and 0.5 mg was chosen. And then, (B) the amount of PVP as dispersing agents, as well as a blocker, was increased. (C) For decreasing excess single AgNPs, the amount of AgNO<sub>3</sub> was reduced, resulting in an incomplete Ag shells. (D) More homogeneous shell formation was induced by changing the kind of reducing agent.

**Table S3.** Detail structure of AgNSs by Si NP core sizes. (mean±S.D., n = 20)

Sample name	Si NP core size (nm)	Final AgNS size (nm)	Thickness of Ag shell (nm)
AgNS (I)	59.3 ± 3.9	118.7 ± 25	29.7 ± 7
AgNS (II)	82.0 ± 12.3	151.6 ± 10	34.8 ± 4
AgNS (III)	103.0 ± 12.0	164.6 ± 11	30.8 ± 6
AgNS (IV)	123.7 ± 12.1	185.5 ± 12	31.4 ± 5
AgNS (V)	147.9 ± 7.1	207.2 ± 7	29.7 ± 5

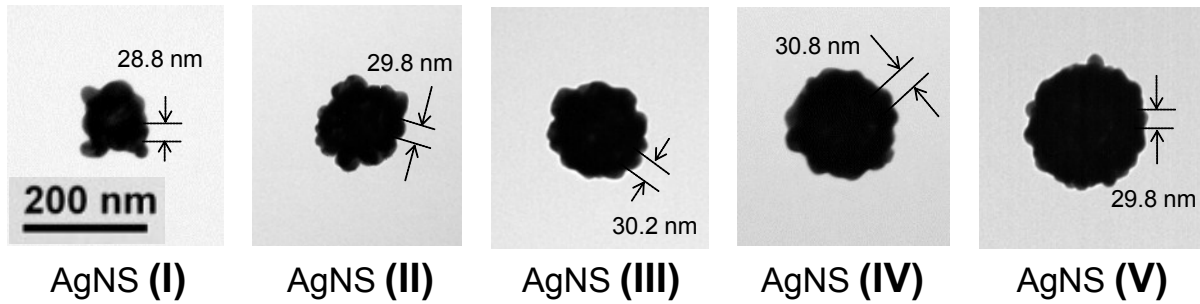
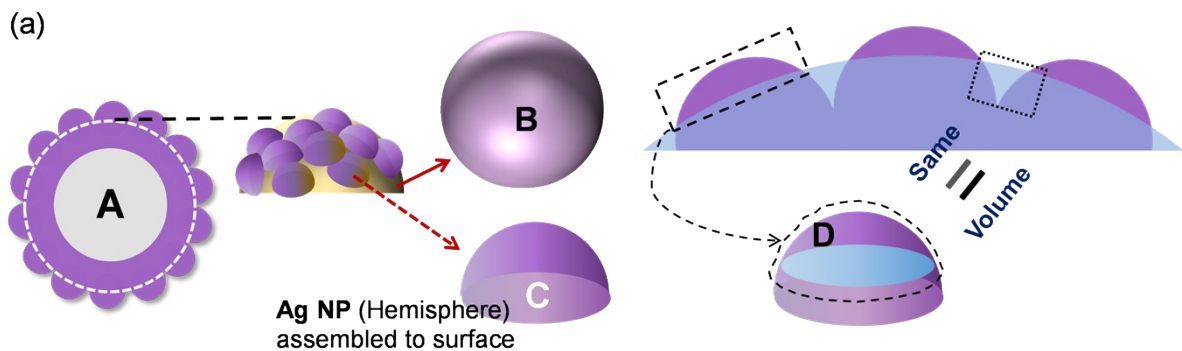


**Fig. S3.** Measurement of diameters of Ag NPs on AgNSs. The two arrows in each TEM image indicate the size of Ag NP assembled on the Si NP core. We measured 20 particles of Ag NPs and calculated the average size in each sample.



(b) **The number (a) of Ag NP assembled to surface**  

$$= \frac{\text{The surface area of particle indicated with white dotted line B}}{\text{Cross sectional area of Ag NP C}}$$

**The volume of A**  

$$= \text{The volume of B} + (a) \times \text{the volume of C}$$

**Sum of deviation volumes**  

$$= \text{Total volume above the mean line sphere} + \text{The total valley space volume of AgNS under MLS}$$

$$= 2 \times (\text{Total volume of D})$$

$$= 2 \times [(a) \times \text{The single volume of D}]$$

**Fig. S4.** The evaluation method of the roughness factor of AgNSs. (a) Illustrations show the detailed modeling of bumpy AgNSs. The particle A is composed of a sphere B and several hemispheres C assembled to a surface of B. D in the dotted box indicates the volume of AgNS above the mean line sphere. The total volume of D is same as the total volume of AgNS below the mean line sphere. (b) The calculating method of the volume of A and deviation volumes using modeling of (a).

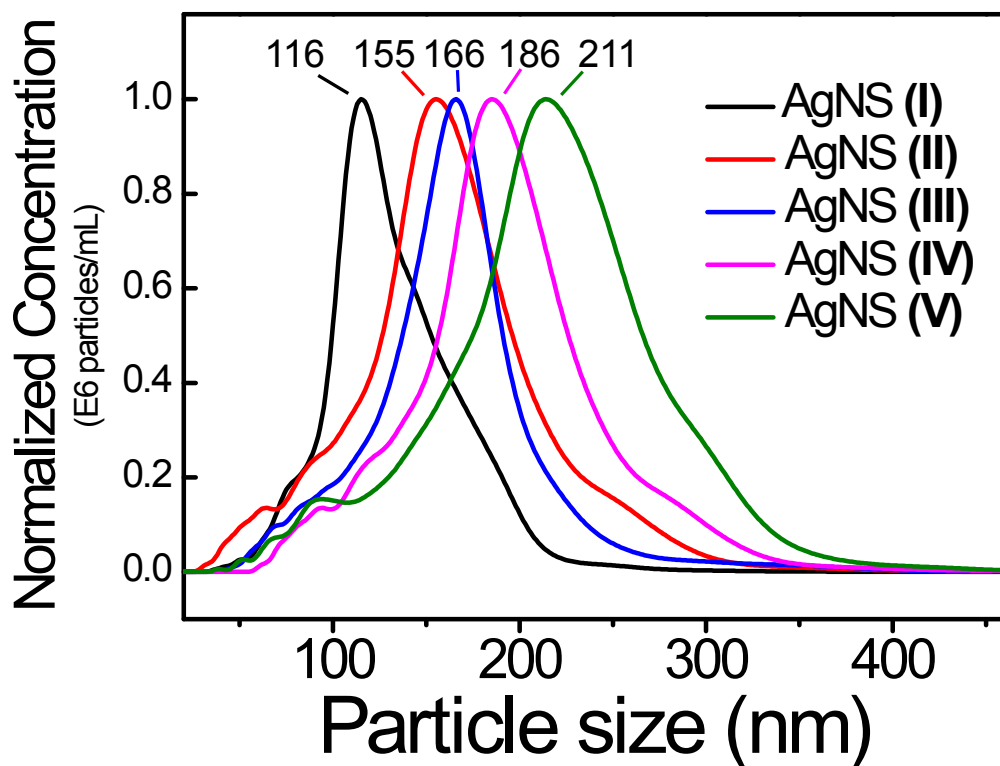


**Fig. S5.** The size distributions of 4-FBT labeled AgNS (I) – (V) measured by Nanoparticle Tracking Analysis (NTA). The numbers written above the plots correspond to mode of particle size (I) – (V). The mode size analyzed by the NTA instrument is similar to the value of Figure 2c. All the plots shown in the graph had an even distribution of the mode value of the particle size.

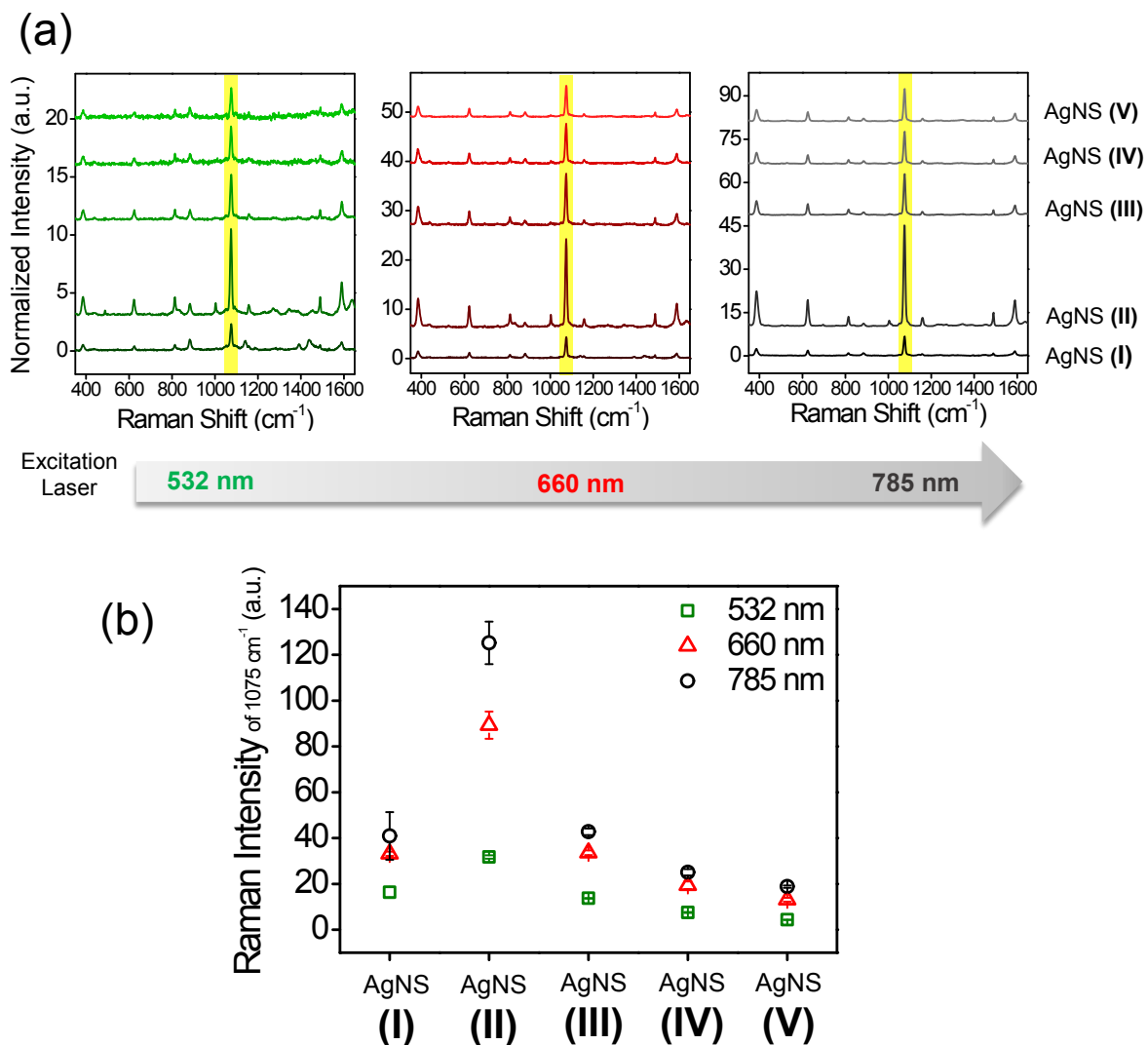


**Fig. S6.** Analysis of SERS properties of AgNSs in solution with different excitation lasers. (a) Typical SERS spectra of 4-fluorobenzenethiol (4-FBT) supported on the AgNSs (I) – (V) using three different excitation lasers of 532 nm (8.3 mW), 660 nm (6.6 mW), and 785 nm (10.0 mW). All spectra were obtained in ethanol by 1 s acquisition and normalized with 882  $\text{cm}^{-1}$  bands (a typical ethanol band). The yellow regions correspond to the intensity at 1075  $\text{cm}^{-1}$  of the SERS spectra, and the intensities of those peaks were analyzed in (b). (b) SERS intensities of the peak at 1075  $\text{cm}^{-1}$  per relative surface area for the Ag NSs of various sizes (I) – (V) at three excitation wavelengths (532, 660, and 785 nm).

### ***Calculation of the SERS enhancement factor (EF)***

SERS enhancement factor (EF) for the AgNS can be calculated using the following equation:

$$EF = (I_{\text{SERS}}/N_{\text{SERS}}) \div (I_{\text{normal}}/N_{\text{normal}})$$

where  $I_{\text{SERS}}$  and  $I_{\text{normal}}$  are the intensities of a Raman band from SERS and normal Raman scattering, respectively, and  $N_{\text{normal}}$  and  $N_{\text{SERS}}$  are the numbers of 4-FBT in pure form and self-assembled on the surface of AgNS, respectively. The Raman band at  $1075 \text{ cm}^{-1}$  for 4-FBT was used to estimate the EF. AgNS nanoparticle dispersed on a patterned slide glass and neat 4-FBT (liquid) are used for measuring  $I_{\text{SERS}}$  and  $I_{\text{normal}}$ , respectively, using identical laser power with  $\times 100$  objective lens (NA 0.90) for the EF calculation. Especially, the AgNS samples were dropped on a patterned slide glass, and SERS spectra were measured by point-by-point mapping with a  $1\text{-}\mu\text{m}$  step size to obtain the values of  $I_{\text{SERS}}$ . After the SERS measurement, SEM images of the same area were obtained using a field emission scanning electron microscope for single particle-based analysis. To obtain  $N_{\text{normal}}$ , light collection volume of  $18.8 \mu\text{m}^3$  was approximated from a cylindrical illuminated volume with  $2 \mu\text{m}$  diameter and  $6 \mu\text{m}$  height for normal Raman measurements. The molecular weight and density of 4-FBT are  $125.2 \text{ g/mol}$  and  $1.203 \text{ g/cm}^3$ , respectively, and hence  $N_{\text{normal}}$  was estimated  $1.09 \times 10^{11}$ .  $N_{\text{SERS}}$  was estimated by considering the surface area of spherical nanoparticle (AgNS is assumed as spherical shape) and a molecular footprint of 4-FBT ( $0.383 \text{ nm}^2/\text{molecule}$ )<sup>2</sup> covering the whole surface of AgNS. Thus,  $N_{\text{SERS}}$  of AgNS was approximately  $5.21 \times 10^4$ ,  $9.67 \times 10^4$ ,  $1.18 \times 10^5$ ,  $1.58 \times 10^5$ , and  $2.06 \times 10^5$  in the case of 60 nm, 80 nm, 100 nm, 120 nm, and 150 nm of AgNS, respectively. The laser power was controlled at sub-mW level with slight difference (1.2 mW for 532 nm, 1.6 mW for 660 nm, and 1.8 mW for 785 nm). However, the difference of laser power was cancelled out since the same laser power was used for normal Raman and SERS measurement at each wavelength of incident photo-excitation.

**Table S4.** The size of Ag NP assembled on Si NP core and calculation of roughness elements from bumpy AgNS particles. (mean±S.D., n = 20)

<b>Sample</b>	<b>Size of Ag NP assembled on Si NP core (nm)</b>	<b>Volume of AgNSs (nm<sup>3</sup>)</b>	<b>Surface area of mean line sphere (nm<sup>2</sup>)</b>	<b>Total deviation volume (nm<sup>3</sup>)</b>	<b>Roughness</b>
AgNS (I)	<b>29.6</b>	616446.20	35027.91	123397.46	<b>0.067</b>
AgNS (II)	<b>30.2</b>	1402910.21	60604.38	212864.06	<b>0.051</b>
AgNS (III)	<b>30.2</b>	1879527.30	73651.77	256323.05	<b>0.045</b>
AgNS (IV)	<b>30.3</b>	2721657.66	94269.92	325464.04	<b>0.040</b>
AgNS (V)	<b>29.8</b>	3905298.18	119927.91	402098.70	<b>0.034</b>

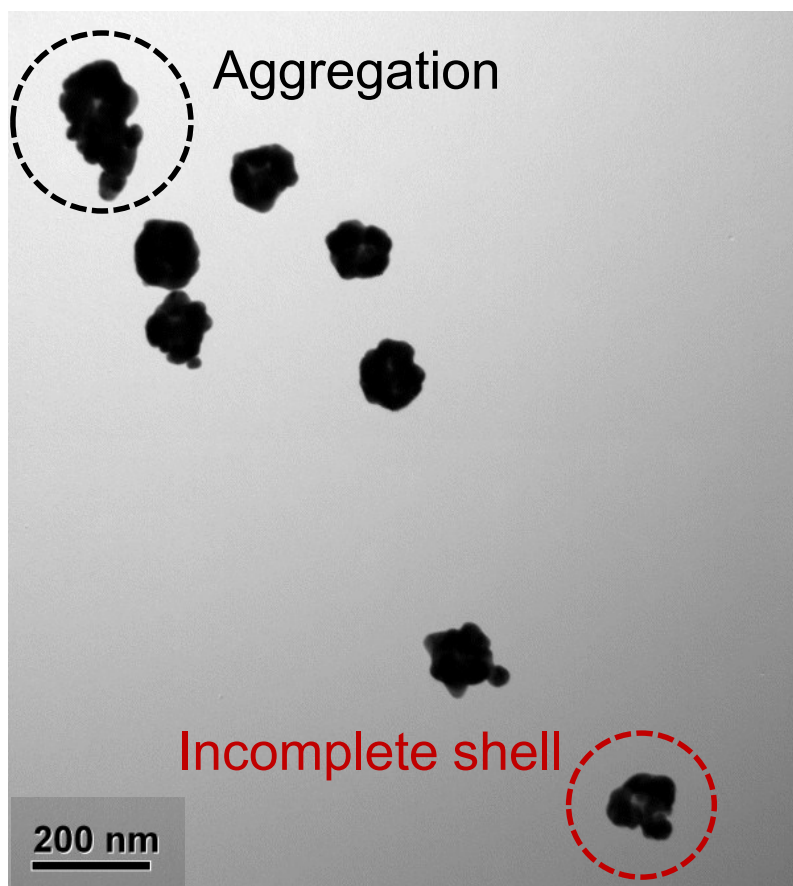


**Fig. S7.** The TEM image of AgNS (I). Black dotted circle indicates aggregation of particles. The red circle indicates the incomplete shell of the particles. Because of the small size, AgNS (I) has relatively unstable structure compared to the other sized particles.

## References

1. H. Kang, J. Yim, S. Jeong, J.-K. Yang, S. Kyeong, S.-J. Jeon, J. Kim, K. D. Eom, H. Lee and H.-I. Kim, *ACS Appl. Mater. Interfaces*, 2013, **5**, 12804-12810.
2. P. Jiang, K. Deng, D. Fichou, S. S. Xie, A. Nion and C. Wang, *Langmuir*, 2009, **25**, 5012-5017.